

Dextran Modified Silicon Photonic Microring Resonator Sensors

Jessie Yiyang Quah , Vivian Netto , Jack Sheng Kee , Eric Mouchel La Fosse , Mi Kyoung Park

Abstract—We present a dextran modified silicon microring resonator sensor for high density antibody immobilization. An array of sensors consisting of three sensor rings and a reference ring was fabricated and its surface sensitivity and the limit of detection were obtained using polyelectrolyte multilayers. The mass sensitivity and the limit of detection of the fabricated sensor ring are 0.35 nm/ng mm⁻² and 42.8 pg/mm² in air, respectively. Dextran modified sensor surface was successfully prepared by covalent grafting of oxidized dextran on 3-aminopropyltriethoxysilane (APTES) modified silicon sensor surface. The antibody immobilization on hydrogel dextran matrix improves 40% compared to traditional antibody immobilization method via APTES and glutaraldehyde linkage.

Keywords—Antibody immobilization, Dextran, Immunosensor, Label-free detection, Silicon micro-ring resonator

I. INTRODUCTION

SILICON photonic microring resonators are an emerging label-free sensing technology that has recently been under intensive investigation [1-4]. Silicon microring resonators are extremely attractive as a biosensor due to their extremely small footprint and high sensitivity [5]. They can be integrated into a compact array, provide multiplexed detection within a single device and readily combined with fluidic components. In addition, monolithic integration of sensor with CMOS electronics is also feasible. The combination of low-cost fabrication and high sensitivity through small dimensions makes micro-ring resonator a good candidate for disposable biosensor chips.

Silicon ring resonators are essentially refractive index-based (RI) sensors. Briefly, in a ring resonator, light coupled by means of an adjacent linear waveguide is strongly localized around the circumference of the microring under conditions of optical resonance, as defined by the cavity geometry and the surrounding RI environment. Biomolecule binding events (i.e. antibody-antigen interaction) on the surface of the micro-ring lead to an increase in the effective RI and a shift in the resonant wavelength. The resonant wavelength shifts ($\Delta\lambda$) proportionally with the mass change of analytes bound to the surface according to an interferometric-based condition:

$$\Delta\lambda = \frac{\Delta n_{eff} \cdot \lambda_{res}}{n_g} \quad (1)$$

Jessie Yiyang Quah and Mi Kyoung Park are with Bioelectronics Program, Institute of Microelectronics, A*STAR (Agency for Science, Technology and Research), Singapore 117685 (e-mail: parkmk@ime.a-star.edu.sg).

Vivian Netto and Eric Mouchel La Fosse are with Aptilus, Pte Ltd., 25 International Business Park, Singapore (e-mail: eric@aptilus.com).

where Δn_{eff} is the change of the effective refractive index caused by analyte binding, λ_{res} is the initial resonance wavelength, and n_g is the group index [6]. Therefore, by directly monitoring the resonant wavelength shift of a microring, it is possible to obtain quantitative information about the binding of molecules near the surface. Silicon microring resonators typically exhibit a high Q factor ($>10^5$) owing to the geometry and the extremely low surface roughness. Their resonance peaks become extremely spectrally narrow which facilitate high resolution in terms of the spectral shift. This makes these devices very sensitive to the local refractive changes near the surface. Micro-ring based biosensors have demonstrated highly sensitive and label-free detection of proteins [7-8], lectins [9] and nucleic acid sequences [10].

The immobilization of antibodies on sensor chips plays a very important role in the performance of a biosensor as an immunoassay platform. A variety of silane chemistries have been widely used to facilitate the immobilization of biomolecules on silicon based biosensors, for example, the use of amino silane and glutaraldehyde linkage to immobilize antibodies. However, because of these two-dimensional (2D) structures, the immobilization capacity is limited, which results in relatively low sensitivity of sensors. One of the ways to overcome this problem is to coat a hydrogel matrix on top of the sensor surface, providing long and hydrophilic spacer arms with reaction sites for immobilization of antibodies or other types of ligands.

In this study, we describe the modification of silicon microring resonator sensors with a hydrogel matrix of dextran. First, sensor characteristics such as sensitivity, repeatability, and detection limit were investigated by depositing polyelectrolyte multilayers (PEMs) of PSS/PAH bilayers. Then, the effect of the degree of oxidation of dextran on the thickness of modified dextran matrix and the antibody immobilization capacity are investigated in detail for surface charge and cross-link density.

II. EXPERIMENTAL

A. Materials

Alpha Thrombin (human, M.W. = 37 kDa) and polyclonal sheep antibody to human thrombin were purchased from Abcam (Hong Kong) Ltd. 3-aminopropyltriethoxysilane (APTES), dextran (Mw = 141K), sodium periodate, 99% (NaIO₄), glutaraldehyde solution (50% wt in water), sodium cyanoborohydride solution (5.0 M in 1 M NaOH), ethanolamine were purchased from Sigma-Aldrich (St. Louis, MO).

Poly (sodium-4-styrenesulfonate) and poly (allylamine hydrochloride) were also purchased from Sigma-Aldrich. Other chemicals were analytical reagent grade and used as received. All samples and buffers were prepared using deionized water obtained from a Milli-Q water purification system.

B. Microring Resonator Sensor

Microring structures, waveguides, and gratings were patterned on commercially available 200 mm SOI wafer with 220 nm-thick top silicon layer and 2 μm -thick buried oxide layers by 248 nm deep UV lithography and etched to buried oxide layer by reactive ion etching (RIE) process, followed by the deposition of 1.5 μm PECVD SiO_2 as a top cladding layer. An array of micro-rings consists of four rings that are connected to one common input waveguide (through) and each ring has a dedicated output waveguide (drop). Three of these four rings are sensor rings where windows are opened over selected individual sensor ring via the combination of dry and wet etching. One of the rings is a reference sensor to monitor temperature induced drift. The chip layout is illustrated in Fig. 1.

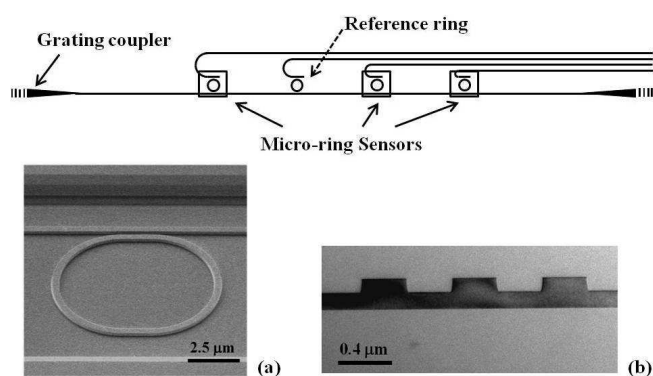


Fig. 1 The layout of an array of SOI micro-ring sensors and TEM images of (a) sensor ring and (b) grating coupler

The rings are race-track style rings with radius 5 μm , and coupling length varies from 2 μm to 2.042 μm to avoid spectral overlap of resonances. A typical TEM image of a micro-ring is shown in Fig 1(a). The waveguide dimensions are 220 nm \times 500 nm and the gap between linear waveguide and ring is 220 nm. A typical spectrum of a sensor has $Q = 24,000$ and $\text{FSR} = 17$ nm. Light from an external near-IR tunable laser (1510 nm – 1570 nm) which is passed through an inline polarization controller is coupled into a vertical grating coupler located at one end of a linear waveguide. The output signals of the three rings are collected via a vertical grating coupler (10°) to single-mode fiber optic probe. Insertion loss (IL) spectrum was measured with EXFO IQS-12004B DWDM passive component test system.

C. APTES surface preparation

To remove any residual organic contaminants, silicon microring sensor chips were first cleaned by a 30 min immersion in piranha solution (2:1 H_2SO_4 :30% H_2O_2) and are then rinsed with copious amounts of water and dried under a stream of nitrogen.

The silicon microring device was then treated with oxygen plasma. Then it was immersed in a solution of 2% 3-aminopropyltriethoxysilane (APTES) in a mixture of ethanol/ H_2O (95%/5%, v/v) for 2 hours followed by thoroughly rinsing with ethanol and DI water, drying under a nitrogen stream, and heated at 120 $^\circ\text{C}$ for 15 min.

D. Polyelectrolyte Deposition

Polyelectrolyte multilayer film was built by alternately immersing the APTES modified device in aqueous solutions of poly (sodium-4-styrenesulfonate) (PSS, 1 mg/mL in 50 mM NaCl) and poly (allylamine hydrochloride) (PAH, 1 mg/mL in 50 mM NaCl) for 15 min each. After each polymer deposition, the device was rinsed three times in DI water and followed by nitrogen drying for measurement in air.

E. Dextran Modification

First, an oxidized Dextran solution was prepared by mixing 30 μmol (repeat unit) of dextran with 60 μmol of sodium periodate in 600 μL of water at room temperature. The solution was stirred in the dark for a given time. To an oxidized dextran solution, 6 μL of 5 M NaBH_3CN solution was added and 5 μL of 0.67 M of sodium borate buffer was added to adjust pH to 7.0. 100 μL of mixed solution was immediately applied on the APTES modified sensor chip in a petri dish and left in the dark overnight. The dextran modified chip was then rinsed with ultrapure water and dried under a nitrogen stream.

F. Antibody immobilization

50 μL of 100 $\mu\text{g}/\text{mL}$ polyclonal anti-thrombin antibody in 50 mM MES buffer (pH 6.0) with 20 mM NaBH_3CN was applied on the dextran modified sensor chip. The sensor chip was incubated overnight in 4 $^\circ\text{C}$. The antibody immobilized chip was then rinsed with MES buffer and dried under a nitrogen stream.

III. RESULTS AND DISCUSSIONS

A. Surface Sensitivity

The resonant wavelength shift versus the number of deposited bilayers is shown in Figure 2. One cycle of PSS and PAH deposition is referred as one bilayer. First, the resonant spectrum was taken in air after each bilayer deposition. The resonant wavelength shifts from three sensor rings are much closed to each other while the shift from the reference ring is negligible. The linear fitting shows that for each layer of PSS/PAH change, the resonance red shift is ~ 0.70 nm. The sensitivity for surface mass detection is given by $S_m = \Delta\lambda/\sigma_p$, where σ_p is the surface density of polyelectrolyte film. The thickness of each polymer bilayer is a function of sodium chloride concentration used in polymer solution preparation. The theoretical thickness of one bilayer of PAH/PSS is ~ 1.7 nm in 50 mM of sodium chloride [11]. In order to verify the thickness of the coated polymer, the samples are prepared by Focused Ion Beam (FIB), and the thicknesses are measured from TEM images. After coating of 6 bilayers of PEMs, the measured thickness of the PEMs is 9.8 nm which is in good agreement with the 10.2 nm of theoretical thickness of 6 bilayers.

The density of polyelectrolyte multilayer is known to be $1.2 \times 10^6 \text{ g/m}^3$ [11]. Therefore the surface density is $\sim 2.0 \text{ ng/mm}^2$ for each period of the PSS/PAH layer. Using the value of the resonance shift from this experiment, we calculate a mass sensitivity of $S_m = 0.35 \text{ nm/ng mm}^2$. The detection limit (L_m) can be obtained by $L_m = R/S_m$, where R is sensor resolution related to system noise and S_m is the surface sensitivity and the detection limit of the fabricated sensor is calculated to be $L_m = 42.8 \text{ pg/mm}^2$. The obtained values are comparable to those reported in previous literature. Since the detection limit is defined by the system noise (mainly from the resolution of the tunable laser), it can be further improved by reducing noise of the system by optimizing the device and measurement instruments.

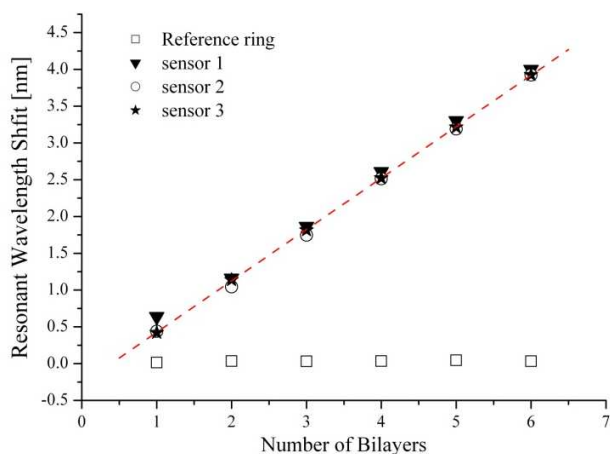


Fig. 2 Resonant wavelength shift versus the number of bilayers (n) after the deposition of (PSS/PAH) n

B. Dextran Modification

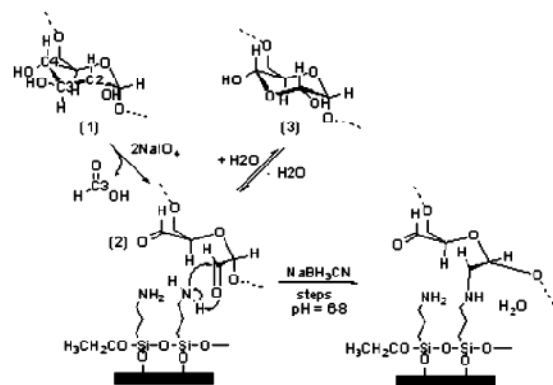


Fig. 3 Reaction scheme for oxidation of dextran and subsequent grafting to APTES modified silicon dioxide surface

In order to covalently attach dextran molecules on APTES modified sensor surface, the polysaccharides were activated by oxidation of anhydroglucopyranoside subunits by NaIO_4 producing the dialdehyde (Fig. 3). Dialdehyde could then be reacted with amine groups on the sensor surface to form a Schiff base linkage. Such linkages are unstable and can dissociate again. They were therefore stabilized by reduction to amine linkages using sodium cyanoborohydride (NaBH_3CN).

The resonant wavelength shift of APTES modified microring resonator sensor after the modification of dextran depends on the molar ratios of NaIO_4 to dextran repeating units and on the reaction time (Fig. 4). The amount of dextran brushes formed on the sensor surface can be controlled by varying the concentration of aldehyde subunits along the dextran backbone. When the degree of oxidation time is shorter, the amount of grafted dextran brushes increases.

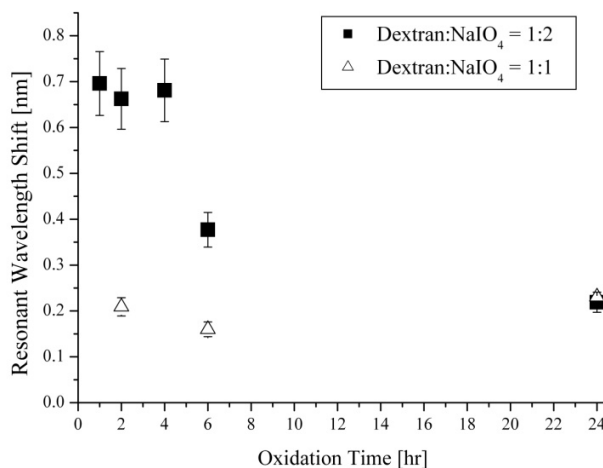


Fig. 3 Resonant wavelength shift of dextran modified silicon microring resonator sensors as a function of oxidation times for different molar ratios of dextran to NaIO_4

Namely, at low oxidation (i.e., 0.5 h), individual dextran molecules form relatively few bonds with surface sites, because the number of oxidized glucopyranoside subunits per molecule is low. Because molecules are strongly hydrated and extend away from the substrate (i.e., polymer brush), many dextran molecules are able to access the surface sites to produce a high grafting density of molecules per surface area. As percent oxidation increases, many surface sites react with a single molecule resulting in a more tightly bound molecule and a lower grafting density.

C. Antibody Immobilization

TABLE I
 RESONANT WAVELENGTH SHIFT AFTER ANTI-THROMBIN ANTIBODY
 IMMOBILIZATION AT VARIOUS OXIDATION CONDITIONS

	Dextran oxidation time [hr]	Further oxidation time [hr]	Resonant wavelength shift [nm]
Without further oxidation	1	-	1.16
	2	-	1.55
	4	-	0.87
Further oxidation	2	4	1.16
	2	16	0.39
APTES/GAD chemistry	-	-	1.09

ACKNOWLEDGMENT

This work was supported by the Agency for Science Technology and Research (A*STAR) Joint Council Office (JCO) grant, Singapore, under Grant No. JCOAG03_FG07_2009.

REFERENCES

- [1] A. L. Washburn, R. C. Bailey, "Photonics-on-a-chip: recent advances in integrated waveguides as enabling detection elements for real-world, lab-on-a-chip biosensing applications," *Analyst*, vol. 126, pp. 227-236, 2010.
- [2] K. De Vos, I. Bartolozzi, E. Schacht, P. Bienstman, R. Baets. "Silicon-on-Insulator microring resonator for sensitive and Label-free Biosensing," *Optical Express*, v.15, pp. 7610-7615, June 2007.
- [3] C. F. Carlborg, K. B. Gylfason, A. Kazmierczak, F. Dortu, M. J. Bañuls Polo, A. Maquieira Catala, et al. "A packaged optical slot-waveguide ring resonator sensor array for multiplex label-free assays in labs-on-chips," *Lap on a Chip*, vol. 10, pp. 281-290, 2010.
- [4] A. Densmore, M. Vachon, D.-X. Xu, S. Janz, R. Ma, Y.-H. Li, et al. "Silicon photonic wire biosensor array for multiplexed real-time and label-free molecular detection," *Optics Letters*, vol. 34, pp.3598-3600, December 2009.
- [5] S. Mandal and D. Erickson, "Nanoscale optofluidic sensor arrays," *Opt. Express*, vol. 16, pp. 1623-1631, February 2010.
- [6] M. Iqbal, M. A. Gleeson, B. Spaugh, F. Tybor, W. G. Gunn, M. Hochberg, et al. "Label-Free Biosensor Arrays Based on Silicon Ring Resonators and High-Speed Optical Scanning Instrumentation," *IEEE J. Sel. Top. Quantum Electronics*, vol.16, pp. 654-661, May/June 2010.
- [7] A. L. Washburn, M. S. Luchansky, A. L. Bowman, R. C. Bailey, "Quantitative, Label-Free Detection of Five Protein Biomarkers Using Multiplexed Arrays of Silicon Photonic Microring Resonators," *Anal. Chem.*, vol. 82, pp. 69-72, 2010.
- [8] A. J. Qavi, J. T. Kindt, M. A. Gleeson, R. C. Bailey, "Anti-DNA:RNA Antibodies and Silicon Photonic Microring Resonators: Increased Sensitivity for Multiplexed microRNA Detection," *Anal. Chem.*, vol. 83, pp. 5949-5956, 2011.
- [9] J.-O. Lee, H.-M. So, E.-K. Jeon, H. Chang, K. Won, Y. H. Kim, "Aptamers as molecular recognition elements for electrical nanobiosensors," *Anal. Bioanal. Chem.* Vo. 390, pp. 1023-1032, 2008.
- [10] Z. Feldötö, I. Varga, E. Blomberg, "Influence of salt and rinsing protocol on the structure of PAH/PSS polyelectrolyte multilayers," *Langmuir*, vol.126, pp. 17048-17057, 2010.
- [11] F. Caruso, K. Niikura, D.N. Furlong, Y. Okahata, I. Ultrathin multilayer polyelectrolyte films on gold: construction and thickness determination, *Langmuir*, 13 (1997) 3422-3426.